IEEE Access
Multidisciplinary | Rapid Review | Open Access Journal

Received June 11, 2018, accepted July 20, 2018, date of publication August 2, 2018, date of current version September 7, 2018.

Digital Object Identifier 10.1109/ACCESS.2018.2862862

Design and Analysis of an OFDM-Based Orthogonal Chaotic Vector Shift Keying Communication System

FADHIL S. HASAN[1] AND ALEJANDRO A. VALENZUELA[2]
[1]Electrical Engineering Department, Al-Mustansiryah University, Baghdad 14150, Iraq
[2]EMT Department, Hochschule Bonn-Rhein-Sieg University of Applied Sciences, 53757 Sankt Augustin, Germany
Corresponding author: Fadhil S. Hasan (fadel_sahib@uomustansiriyah.edu.iq)

ABSTRACT We propose a new non-coherent multicarrier spread-spectrum system that combines orthogonal chaotic vector shift keying (OCVSK) and orthogonal frequency-division multiplexing (OFDM). The system enhances OCVSK by sending multiple groups of information sequences with the same orthogonal chaotic vector reference sequences over the selected subcarriers. Each group carries M information bits and is separated from other groups by orthogonal chaotic reference signals. We derive the information rate enhancement (IRE) and the energy saving enhancement (ESE) factors as well as the bit error rate theory of OFDM-OCVSK under additive white Gaussian noise and multipath Rayleigh fading channels and compare the results with conventional OCVSK systems. For large group numbers, the results show that the IRE and ESE factors approach $\mathrm{M}\times 100\%$ and $\mathrm{M}/(\mathrm{M}+1)\times 100\%$, respectively, and thus outperform OCVSK systems. The complexity analysis of the proposed scheme as compared with OFDM-DCSK shows a significant reduction in the number of complex multiplications required.

INDEX TERMS Orthogonal chaotic vector shift keying, orthogonal frequency division multiplexing, OFDM-based DCSK, OFDM-based SR-QCSK, energy efficiency, high information rate, performance analysis, complexity analysis.

I. INTRODUCTION

Over the past decade, chaos-based wireless digital communication systems have attracted increasing research interest [1]. The sensitivity of chaotic signals to initial conditions allows infinite numbers of independent signals to be generated easily at low cost, with high security and a good degree of randomness. Furthermore, chaotic systems have a large bandwidth, low power spectral density and immunity against multipath fading channels [2] and jamming coupled with a low probability of interception [3]. One of the most popular non-coherent chaos modulation techniques for communication systems is differential chaos shift keying (DCSK) [2]. Unlike coherent chaos shift keying (CSK) [4], DCSK is able to detect the transmitted bits without requiring any synchronization or channel state information (CSI) on the receiver side.

The first proposed DCSK system used two time slots for each transmitted bit [5], with the reference chaotic signal being sent in the first time slot and the data bearing signal in the second. Although the reference signal solved the synchronization problem, it added other problems of its own such as lower data rate, energy efficiency and security. The bit error rate (BER) analysis of DCSK over multipath fading channels was derived in [6] and [39]. In recent years, many researchers have proposed improvements to the weaknesses of DCSK systems [8]–[22]. The transmitter bit energy variant was solved in [8] and [9] using frequency modulated DCSK (FM-DCSK). Several techniques to enhance the data rate and spectral efficiency are proposed in [7] and [10]–[16], including quadrature chaos shift keying (QCSK), orthogonal chaotic vector shift keying (OCVSK), high efficiency DCSK (HE-DCSK), reference modulated DCSK (RM-DCSK), quadrature amplitude modulation DCSK (QAM-DCSK), M-ary DCSK, high data rate code-shifted DCSK (HCS-DCSK) and multilevel code-shifted DCSK (MCS-DCSK). The need to introduce a delay component for synchronization was solved with code-shifted DCSK (CS-DCSK) [17] and code-shifted QCSK (CS-QCSK) [18] using Walsh codes that allow both the reference and information-bearing signal to be transported in the same time slot. Further ways to improve the information rate by reducing the effect of

reference sequences are those proposed in phase separated DCSK (PS-DCSK) [19], improved DCSK (I-DCSK) [20], short reference DCSK (SR-DCSK) [21], orthogonal multi-level DCSK (OM-DCSK) [22], commutation code index DCSK (CCI-DCSK) [23] and initial condition-index chaos shift keying [24]. Improvements to the security aspect of DCSK using permutation techniques include permutation-based DCSK (P-DCSK) [25] and permutation index DCSK (PI-DCSK) [26]. Kaddoum and Wagemakers design a DCSK system for continuous mobility in [27] and study the lower BER threshold in DCSK systems in [28]. An improvement to OCVSK is proposed in [29] and named amplitude shift keying aided orthogonal chaotic vector PSK (ASK-OCVPSK). Here, the reference chaotic sequence is produced recursively from the shifted orthogonal chaotic vector generated by the Gram-Schmidt algorithm.

Over the past few years, many multicarrier-based DCSK systems have been published that combine multicarrier techniques with DCSK in order to enhance the information rate, energy efficiency, RF delay and bit error rate [30]–[36]. In [30] and [31], Kaddoum *et al.* combine multicarrier techniques with a DCSK (MC-DCSK) system. Li *et al.* [32] study a system that combines orthogonal frequency division multiplexing (OFDM) with DCSK in an AWGN channel and Hasan [33] a combined OFDM and short reference QCSK (SR_QCSK) system in multipath Rayleigh fading channels. Further publications include the combination of MC-DCSK and multi-users such as in multiuser multicarrier differential chaos shift keying (MU MC-DCSK), analogue networking coding-based MC-DCSK (ANC) and multiuser OFDM-based chaos shift keying (MU OFDM-DCSK) in [34]–[36] respectively. Yang *et al.* in particular propose a novel multicarrier chaos shift keying (MC-CSK) modulation system based on multicarrier transmission and multilevel chaos shift keying modulation that depends on orthogonal chaotic vectors and pulse shaping filters.

In orthogonal chaotic vector shift keying (OCVSK) [7], M data bits are sent in the same time slot. Each bit is multiplied by its orthogonal chaotic code sequence and then added together to produce the information-bearing signal. These orthogonal vectors are derived from M reference chaotic signals using the Gram-Schmidt (GS) method on the signals sampled. OCVSK is limited by the length of the reference sequence, which increases in step with the number of data bits carried in the same frame. To overcome this problem, we propose a hybrid OFDM and OCVSK system (OFDM-OCVSK).

II. ORTHOGONAL CHAOTIC VECTOR SHIFT KEYING

Fig. 1 shows the block diagram of an OCVSK modulator. Chaotic generators produce M chaotic signals, each of length β. These chaotic generators can be obtained from the same chaotic attractor with different initial conditions, making them linearly independent [37]. The M chaotic signals of the j^{th} frame $\mathrm{c}^1_{\mathrm{j,k}}, \mathrm{c}^2_{\mathrm{j,k}}, .., \mathrm{c}^{\mathrm{M}}_{\mathrm{j,k}}$ are generated using a second-order Chebyshev polynomial function (CPF) with unity variance

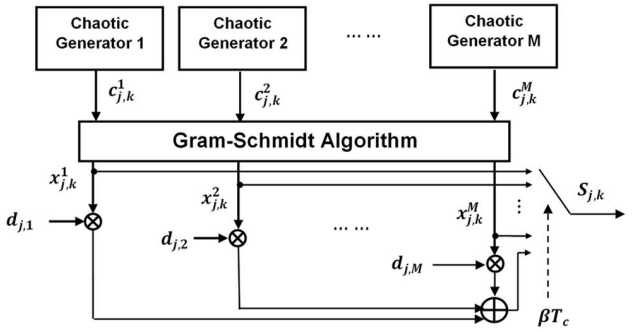

FIGURE 1. OCVSK (orthogonal chaotic vector shift keying) transmitter with M chaotic generators $c^m_{j,k}$ that are converted to perfectly normalized orthogonal chaotic signal codes $x^m_{j,k}$ by the Gram-Schmidt algorithm before spreading the data bits $d_{j,m}$ and being concatenated to produce the OCVSK modulated signal $S_{j,k}$ of length $(M+1)\,\beta$.

and zero mean [33]

$$\mathrm{c_{k+1}} = 1 - 2\mathrm{c_k^2}. \tag{1}$$

The Gram-Schmidt algorithm converts the imperfectly orthogonal chaotic signals to perfectly normalized orthogonal chaotic signals. The m^{th} orthogonal chaotic vectors of the j^{th} frame $\mathrm{x^m_{j,k}}$ can be expressed as [37], [38]

$$x^m_{j,k} = \begin{cases} \dfrac{\mathrm{c^1_{j,k}}}{\sqrt{\sum_{\mathrm{k=1}}^{\beta}\left[\mathrm{c^1_{j,k}}\right]^2}} & for\ m = 1 \\ \dfrac{\mathrm{c^m_{j,k}} - \sum_{\mathrm{q=1}}^{\mathrm{m-1}}\left[\sum_{\mathrm{k=1}}^{\beta}\mathrm{c^m_{j,k}x^q_{j,k}}\right]\mathrm{x^q_{j,k}}}{\sqrt{\sum_{\mathrm{k=1}}^{\beta}\left[\mathrm{c^m_{j,k}} - \sum_{\mathrm{q}}^{\mathrm{m-1}}\left(\sum_{\mathrm{k=1}}^{\beta}\mathrm{c^m_{j,k}x^q_{j,k}}\right)\mathrm{x^q_{j,k}}\right]^2}} & for\ m = 2, 3, \ldots, \mathrm{M} \end{cases} \tag{2}$$

These orthogonal chaotic signals are used as reference sequences that have the total length $M \cdot \beta$. For each j^{th} frame, a serial to parallel circuit converts the information streams$d_{j,m} \in \{1, -1\}/\sqrt{M}$ into M parallel data sequences $\{d_{j,1}, \ldots, d_{j,M}\}$. Each m^{th} data bit $d_{j,m}$ is multiplied by its corresponding m^{th} orthogonal chaotic vector $x^m_{j,k}$ and then totaled to produce the data-bearing signal of length β. The M reference chaotic signals and the information bearing signals are then concatenated to produce the OCVSK modulated signal of length $(M+1)\beta$.

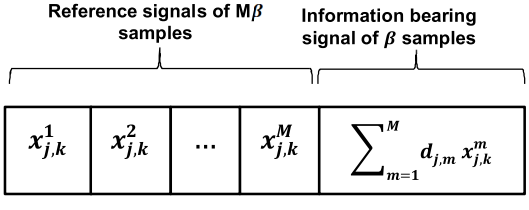

FIGURE 2. OCVSK frame with the M reference chaotic signals located in the first slots and the information-bearing signal in the last slot.

Fig. 2 illustrates the OCVSK frame with the M reference chaotic signals located in the first slots and the information

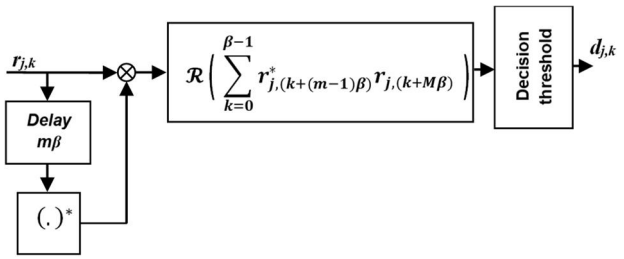

FIGURE 3. OCV-DCSK receiver

bearing signal in the last slot. The OCVSK modulated signal of thej^{th} frame and k^{th} spreading sequence $S_{j,k}$ is expressed as

$$S_{j,k} = \begin{cases} x^1_{j,k} & 0 < k \le \beta \\ x^2_{j,k} & \beta < k \le 2\beta \\ \vdots & \\ x^M_{j,k} & (M-1)\,\beta < k \le M\beta \\ \sum_{m=1}^{M} d_{j,m} x^m_{j,k} & M\beta < k \le (M+1)\,\beta \end{cases} \quad (3)$$

where $x^m_{j,k}$ is the m^{th} reference chaotic signal of the j^{th} frame and k^{th} spreading sequence. The block diagram of the OCVSK receiver is shown in Fig. 3. The received signal of the m^{th} time

slot is denoted as $r_{j,k+(m-1)\beta}$, with $m = 1, 2, \ldots, M+1$. The first reference signal received is then $r_{j,k}$, the second $r_{j,k+\beta}$ and so on up to $r_{j,k+(M-1)\beta}$, which represents the M^{th} reference signal received. The received information-bearing signal is then represented by $r_{j,(k+M\beta)}$. There are therefore M correlation functions that are used to recover the M transmitted bits. The m^{th} correlator of the j^{th} frame is expressed as

$$Z_{j,m} = T_c \sum_{k=0}^{\beta-1} r^*_{j,(k+(m-1)\beta)} r_{j,(k+M\beta)}, \quad (4)$$

with $m = 1, 2, \ldots, M$ and T_c being the chip time. Each m^{th} transmitted bits can be recovered by applying decision thresholds to the real components of $Z_{j,m}$. The original transmitted data stream is obtained from the parallel detected bits after a parallel to serial conversion. OCVSK is limited by the length of the reference signal that occupies $M\beta$ time slots. These reference signals do not carry any information and are only needed for synchronization purposes. To learn more about the effect of M on the bit duration and the transmitted bit energy of OCVSK systems, let us define the bit duration of OCVSK as $T_{b,OCVSK} = (M+1)\,\beta T_c/M$. The transmitted bit energy of the j_{th} frame is then

$$E_{j,b,OCVSK} = \frac{T_c}{M}\left(\sum_{m=1}^{M}\sum_{k=0}^{\beta-1}(x^m_{j,k})^2 + \frac{1}{M}\sum_{m=1}^{M}\sum_{k=0}^{\beta-1}(x^m_{j,k})^2\right) \approx T_c\frac{(M+1)}{M}\beta E\left[\left(x^1_{j,k}\right)^2\right] \quad (5)$$

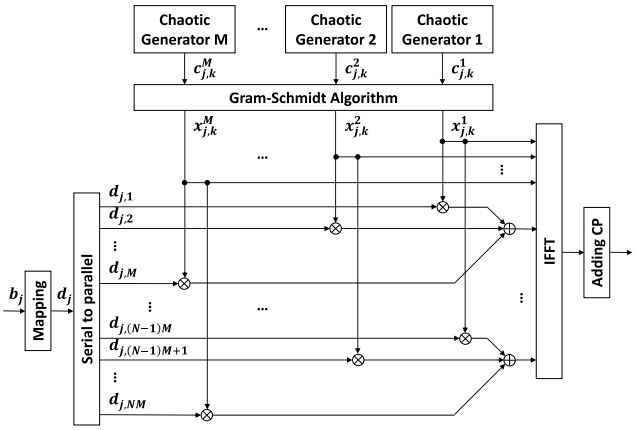

FIGURE 4. OFDM-OCVCSK modulator.

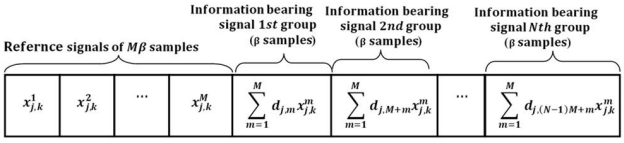

FIGURE 5. OFDM-OCVCSK frame.

where E[.] is the mean function. For $M \gg 1$, $T_{b,OCVSK} \approx \beta T_c$ and $E_{j,b,OCVSK} \approx T_c\beta E\left[\left(x^1_{j,k}\right)^2\right]$ the bit duration and the transmitted bit energy of OCVSK are lower than the bit duration and the transmitted bit energy of DCSK by a factor of two ($T_{b,DCSK} = 2\beta T_c$and$E_{b,DCSK} = 2T_c\beta E\left[x^2_k\right]$ [7]) but similar to the bit duration and the transmitted bit energy of QCSK ($T_{b,QCSK} = \beta T_c$ and $E_{b,QCSK} = T_c\beta E\left[x^2_k\right]$ [10]).

III. OFDM-OCVSK SYSTEM ARCHITECTURE

This section presents the principal design of OFDM-OCVSK systems. Fig. 4 illustrates the block diagram of an OFDM-OCVCSK modulator. Firstly, each stream bit b_j is mapped onto the corresponding symbol $d_j = \{1, -1\}/\sqrt{\mathrm{M}}$.

The serial j^{th} symbol is then converted into M parallel symbols $d_{j,m}$ with $m = 1, \ldots .NM$. The parallel symbols are then divided into N groups, each of M symbols, before they are modulated by the OCVSK modulator. The reference signals are the same for each group. The frame of OFDM-OCVSK consists of M reference chaotic signals, each of length β, giving the reference signals a total length of $M\beta$. The remaining parts of the format are composed of the information chaotic signals that have N groups, each of length β, leading to the total length of the information chaotic signals of $N\beta$. The total length of OFDM-OCVSK frames is therefore $\beta\,(M+N)$ samples with $(N+M)$ slots, where each slot has β samples. Fig.5 shows the structure of the OFDM-OCVSK frame.

Notice that the OFDM-OCVSK system minimizes time and energy compared with the OCVSK system, where $N-1$ reference chaotic signals are needed. The frequency domain of the j^{th} discrete transmitted OFDM-OCVSK signal

$S_j \in R_{(N+M)\times\beta}$ is expressed in matrix form as (6), as shown at the bottom of this page.

Each vector in the k^{th} column of the S_j matrix is modulated using OFDM by taking the inverse FFT in simultaneously with $N_{FFT} = N + M$ subcarriers and selecting the value of N to obtain $N_{FFT} = 2^u$ (u = integer). The format of the transmitted signal is shown in Fig. 6, where the frequency and time domains are represented by the y- and x-axis respectively.

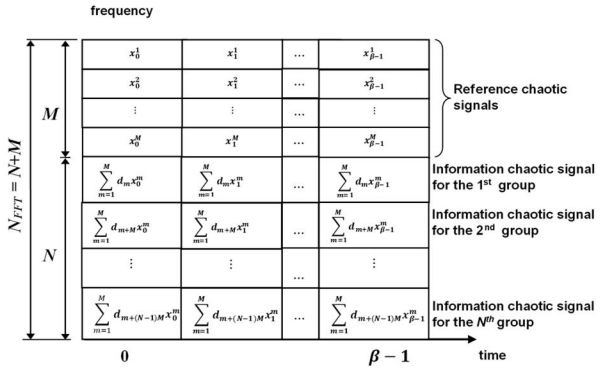

FIGURE 6. Format of signal transmitted by the OFDM-OCVSK signal.

The j^{th} baseband discrete OFDM-OCVSK modulated signal with cyclic extended guard interval is expressed as

$$s_j(k,\upsilon) = \frac{1}{\sqrt{N_{FFT}}} \sum_{n=0}^{N_{FFT}-1} S_j(n,k)\, e^{j2\pi \frac{n\upsilon}{N_{FFT}}}, \quad \upsilon = -N_{guard}, \ldots, N_{FFT}-1 \quad k = 0, \ldots, \beta-1 \tag{7}$$

where N_{guard} is the guard interval, $N_{guard} = \lceil 0.25 N_{FFT} \rceil$, and $\lceil . \rceil$ is the integer operator.

The OFDM-OCVSK receiver block diagram is shown in Fig. 7, where detection is effected without using any channel state information (CSI) or equalization circuit. After removing the cyclic prefix, an FFT is performed for the j^{th} received signal $r_j(k,\upsilon)$

$$R_j(k,n) = \frac{1}{\sqrt{N_{FFT}}} \sum_{\upsilon=0}^{N_{FFT}-1} r_j(k,\upsilon)\, e^{-j2\pi \frac{n\upsilon}{N_{FFT}}}, \quad n = 0, \ldots, N_{FFT}-1 \quad k = 0, \ldots, \beta-1 \tag{8}$$

The j^{th} complex received signal $R_j(k,n)$ is converted into the vector $R_{j,k+(m-1)\beta}$, with $m = 1, \ldots, N+M$ and $k = 0, \ldots, \beta-1$, which represent the reference and information chaotic signals. The reference chaotic signals received are $R_{j,k+(m-1)\beta}$, with $m = 1, 2, \ldots, M$, and are used for all N groups. For each recovered group, there are M correlation functions that are used to detect the M transmitted bits for this group. The overall transmitted bits are $M \cdot N$. To detect the M transmitted bits for the n^{th} group, the conjugates of the m^{th} received reference sequences are multiplied by the n^{th} received information group and then totaled over β sequences in order to get the output of the MNcorrelator according to

$$Z_{j,m}^{n} = T_c \sum_{k=0}^{\beta-1} R_{j,k+(m-1)\beta}^{*} R_{j,k+M\beta+(n-1)\beta}, \quad m = 1, \ldots, M \quad n = 1, \ldots, N \tag{9}$$

where R^* is the conjugate of the R signal. For the j^{th} frame, the m^{th} transmitted bits in each group are then detected by applying a decision threshold to the real components of $Z_{j,m}^{n}$. Finally, a parallel to serial converter changes the NM bits into stream bits.

IV. PERFORMANCE ANALYSIS OF OFDM-OCVSK

In this section, the information rate enhancement (IRE), the energy saving enhancement (ESE) and the transmitted data-energy-to-bit-energy ratio (DBR) factors for OFDM-OCVSK system are derived and compared with other systems such as OFDM-DCSK [32] and OFDM-SRQCSK [33]. The bit error rate (BER) analytic under AWGN and multipath fading channel for OFDM-OCVSK system are also presented.

A. INFORMATION RATE AND ENERGY SAVINGS

$T_{b,OFDM-OCVSK} = (N+M)\,\beta T_c/(NM)$ is first defined as an OFDM-OCVSK bit duration. The information rate enhancement factor IRE of OFDM-OCVSK compared with OCVSK is then written in percentage form as

$$IRE = \left(\frac{T_{b,OCVSK}}{T_{b,OFDM-OCVSK}} - 1 \right) \times 100\% = \frac{M(N-1)}{N+M} \times 100\%. \tag{10}$$

$$S_j = \begin{bmatrix} x_{j,0}^{1} & x_{j,1}^{1} & \cdots & x_{j,\beta-1}^{1} \\ x_{j,0}^{2} & x_{j,1}^{2} & \cdots & x_{j,\beta-1}^{2} \\ \vdots & \vdots & \vdots & \vdots \\ x_{j,0}^{M} & x_{j,1}^{M} & \cdots & x_{j,\beta-1}^{M} \\ \sum_{m=1}^{M} d_{j,m} x_{j,0}^{m} & \sum_{m=1}^{M} d_{j,m} x_{j,1}^{m} & \cdots & \sum_{m=1}^{M} d_{j,m} x_{j,\beta-1}^{m} \\ \sum_{m=1}^{M} d_{j,M+m} x_{j,0}^{m} & \sum_{m=1}^{M} d_{j,M+m} x_{j,1}^{m} & \cdots & \sum_{m=1}^{M} d_{j,M+m} x_{j,\beta-1}^{m} \\ \vdots & \vdots & \vdots & \vdots \\ \sum_{m=1}^{M} d_{j,(N-1)M+m} x_{j,0}^{m} & \sum_{m=1}^{M} d_{j,(N-1)M+m} x_{j,1}^{m} & \cdots & \sum_{m=1}^{M} d_{j,(N-1)M+m} x_{j,\beta-1}^{m} \end{bmatrix} \tag{6}$$

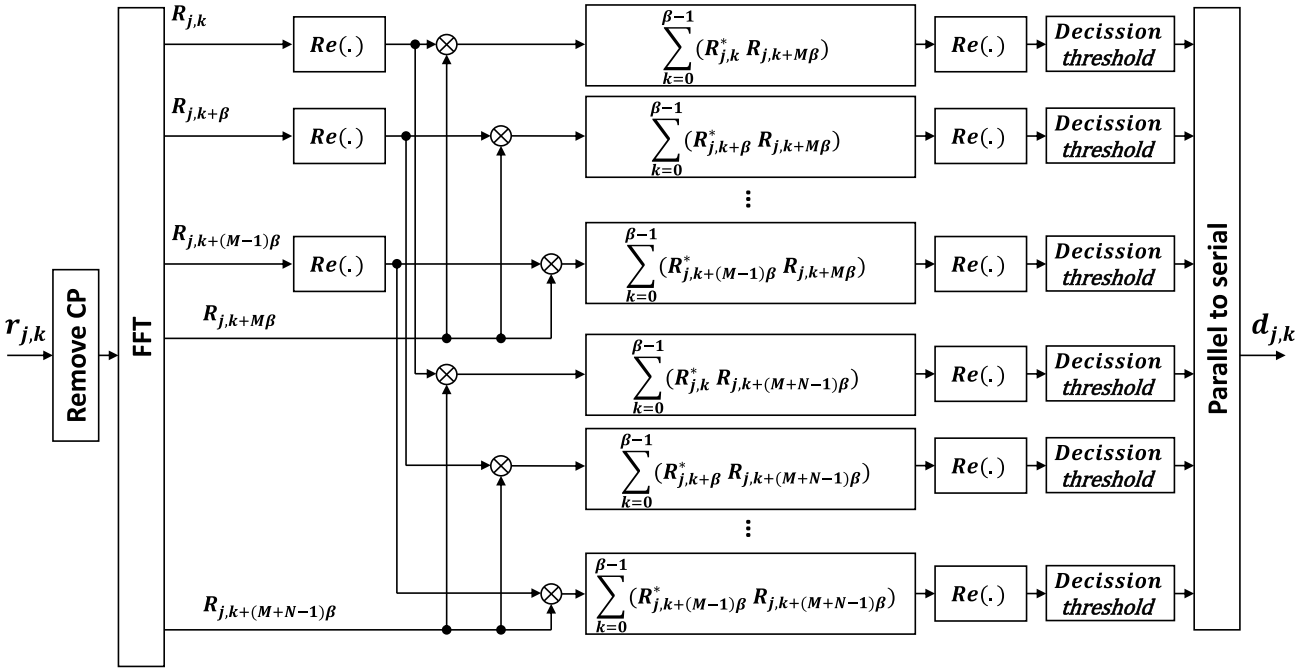

FIGURE 7. OFDM-OCVSK receiver.

$E_{b,OFDM_OCVSK} = T_c\left(\frac{N+M}{NM}\right)\beta E(x_k^2)$ is defined as the OFDM-OCVSK transmitted energy bit, where $E(x_k^2)$ is the mean square value of x_k. The energy saving enhancement factor *ESE* of OFDM-OCVSK compared with OCVSK is then expressed in percentage form as

$$ESE = \left(1 - \frac{E_{b,OFDM-OCVSK}}{E_{b,OCVSK}}\right) \times 100\% = \frac{(N-1)M}{N(M+1)} \times 100\%. \quad (11)$$

In [32] and [33], Li *et al.* and Hasan used the transmitted data-energy-to-bit-energy ratio (DBR) to measure the energy efficiency that is defined as DBR = E_{data}/E_b, where E_{data} is the data energy per bit and E_b is the transmitted bit energy. The energy per bit of OFDM-OCVSK can be expressed in terms of data energy E_{data} and reference energy E_{ref} as

$$E_{b,OFDM-OCVSK} = E_{data} + E_{ref} = E_{data} + \frac{ME_{data}}{N} = \frac{M+N}{N}E_{data}. \quad (12)$$

The DBR of OFDM-OCVSK is then given by

$$DBR = \frac{N}{M+N}. \quad (13)$$

The DBR of OFDM-DCSK [32] and OFDM-SRQCSK [33] are expressed as $N/(N+1)$ and $PN/(PN+2)$ respectively, where *P*is the repeating factor of short reference technique. Figs. 8 and 9 show the *IRE* and *ESE* of OFDM-OCVSK versus N for $M = 2, 4, 8, 16$ and 32. An increasing M will enhance the IRE and ESE factors. For large values of N, IRE and ESE factors approach $M \times 100\%$ and $M/(M+1) \times 100\%$ respectively. For example, when $N = 200$, IRE = 197%, 390%, 765%, 1,474% and 2,744% and ESE = 66%, 79%, 88%, 93% and 96% for $M = 2, 4, 8, 16$ and 32 respectively.

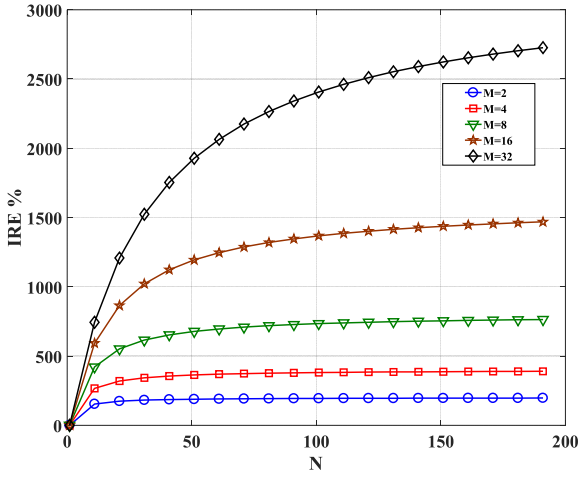

FIGURE 8. Information rate enhancement factor of OFDM-OCVSK versus N for M = 2, 4, 8, 16 and 32.

Fig. 10 shows the DBR of an OFDM-OCVSK system versus N for M = 2, 4, 8, 16 and 32 and compares them with the DBR of an OFDM-DCSK [32] and OFDM-SRQCSK [33] system. As can be seen, increasing M will reduce the DBR factor. Also, the DBR factor of OFDM-SRQCSK is better than all other systems. For large N, the DBR factor approaches 100%. For example, when N = 200, DBR of

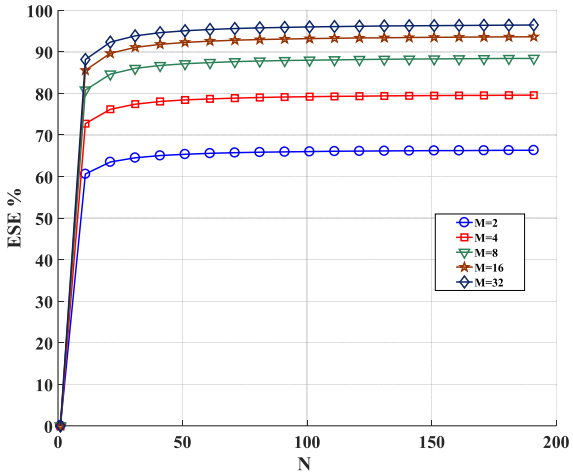

FIGURE 9. Energy saving enhancement factor of OFDM-OCVSK versus N for M = 2, 4, 8, 16 and 32.

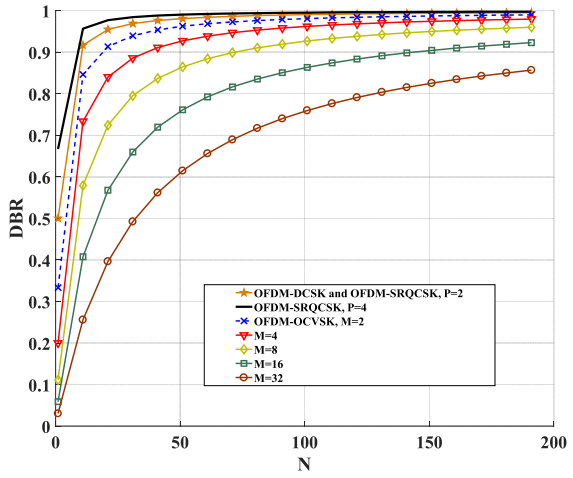

FIGURE 10. DBR for an OFDM-OCVSK system versus N for M = 2, 4, 8, 16 and 32.

OFDM-DCSK $\approx$ 0.995, DBR of OFDM-SRQCSK $\approx$ 0.997 (P = 4) and for OFDM-OCVSK $\approx$ 0.99, 0.98, 0.96, 0.92 and 0.86 for M = 2, 4, 8, 16 and 32 respectively.

B. COMPLEXITY ANALYSIS

The main difference between OFDM-DCSK and OFDM-OCVSK is the GS process employed to generate the M orthogonal sequences that are used to carry the multilevel bits in the same slot. We will therefore focus on the complexity that the GS block introduces on the transmitter side in order to compare the complexity of OFDM-DCSK with that of the proposed system.

The complexity of the GS algorithm in terms of multiplication, addition and division operations for transmitted M $\times$ N bits of data is easy to calculate, only requiring M chaotic vectors, each with lengths of β samples. The numbers of multiplications (MUL), additions (ADD) and divisions (DIV) that are required to generate M orthogonal sequences for each frame only depend on β and M:

$$\begin{aligned} MUL &= (\beta - 1)\left(M^2 + M - 1\right), \\ ADD &= \beta M^2, \\ DIV &= \beta M. \end{aligned} \tag{14}$$

Fig. 11 shows the complexity of the GS algorithm versus M for β = 50 and 100. The complexity increases with M and β, while the number of MUL and ADD operations are approximately the same, in contrast to the small number of DIV operations.

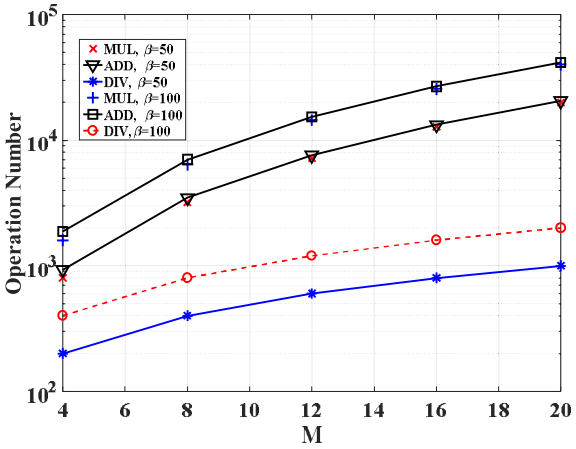

FIGURE 11. Complexity of the Gram-Schmidt process versus M.

TABLE 1. Transmitter complexity of OFDM-DCSK and OFDM-OCVSK.

OFDM-OCVSK			
Operation	**GS**	**OCVSK**	**IFFT**
MUL	βM^2	MN β	$\left(\beta(M+N)\log_2(M+N)\right)^c$
ADD	$(\beta-1)(M^2+M-1)$	(M-1)N β	$\left(\beta\left(\frac{M+N}{2}\right)\log_2(M+N)\right)^c$
OFDM-DCSK			
Operation	**GS**	**DCSK**	**IFFT**
MUL	-	NT β	$\left(\beta(1+N_T)\log_2(1+N_T)\right)^c$
ADD	-	-	$\left(\beta\left(\frac{1+N_T}{2}\right)\log_2(1+N_T)\right)^c$

$(.)^c$ refers to complex operation

Table 1 summarizes the complexities of the OFDM-DCSK and OFDM-OCVSK system on the transmitter side with the three main blocks of GS, chaos modulation and IFFT. The DIV operation is neglected in this comparison. We are assuming that all the subcarriers of the IFFT are fully used by the reference and information chaotic sequences. If N_T represents the number of transmitted bits in each frame for the same number of transmitted bits in both systems, then, for the OFDM-DCSK system, where only one reference is needed, N_{FFT} equals $N_T + 1$, whereas, for the OFDM-OCVSK system, $N_{FFT} = M + N$ and $N_T = M \times N$.

To enable an adequate comparison between the systems, the complex operations were converted to real operations by calculating four real multiplications and two real additions for

each complex multiplication and two real additions for each complex addition. The total complexity of both systems can thus be rewritten as

$$C_{OFDM-DCSK} = \begin{cases} N_T\beta + 4\left(\beta\left(1+N_T\right)log_2\left(1+N_T\right)\right), & MUL \\ 2\left(\beta\left(\dfrac{1+N_T}{2}\right)log_2\left(1+N_T\right)\right) & \\ \quad +2\left(\beta\left(1+N_T\right)log_2\left(1+N_T\right)\right), & ADD \end{cases} \tag{15}$$

and

$$C_{OFDM-OCVSK} = \begin{cases} \beta M^2 + MN\beta + _{MUL-IFFT}, & MUL \\ (\beta-1)\left(M^2+M-1\right) & \\ \quad +(M-1)N\beta + _{ADD-IFFT}, & ADD, \end{cases} \tag{16}$$

where $_{MUL-IFFT}$ and $_{ADD-IFFT}$ are the numbers of multiplications and additions of the IFFT algorithms of OCVSK:

$$C_{MUL-IFFT} = 4\left(\beta\left(M+N\right)log_2\left(M+N\right)\right) \tag{17}$$

$$C_{ADD-IFFT} = 2\left(\beta\left(\frac{M+N}{2}\right)log_2\left(M+N\right)\right) + 2\left(\beta\left(M+N\right)log_2\left(M+N\right)\right). \tag{18}$$

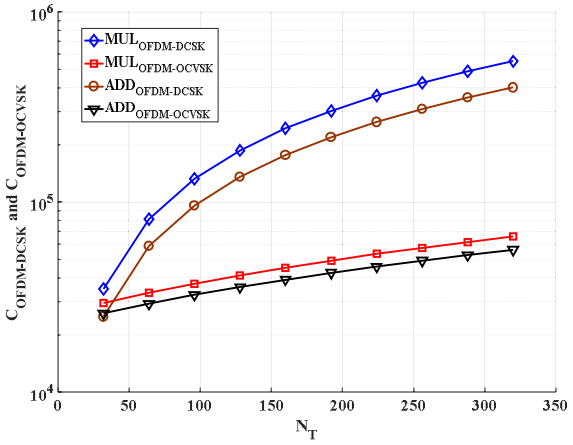

FIGURE 12. Comparing complexity between OFDM-DCSK and OFDM-OCVSK versus transmitted bits per frame for M = 16 and $\beta = 50$.

Fig. 12 shows the total complexity of both systems versus transmitted bits N_T per frame for the same number of transmitted bits and with M = 16 and $\beta = 50$. For larger amounts of transmitted bits, the number of both multiplications and additions is considerably higher in the DSCK compared with the OCVSK system despite the additional GS algorithm in the case of OCVSK. This is because the IFFT algorithm in DSCK is more complex than the GS and IFFT algorithm in OCVSK. Sending 192 bits per frame, for example, will result in $N_T = 193$ for OFDM-DCSK and $N_T = 28$ for OFDM-OCVSK, leading to $7.3 \cdot 10^4$ and $6.7 \cdot 10^3$ complex multiplications.

C. ANALYTIC BER PERFORMANCE

This subsection serves to derive the BER analytics of OFDM-OCVSK under AWGN and multipath slow Rayleigh

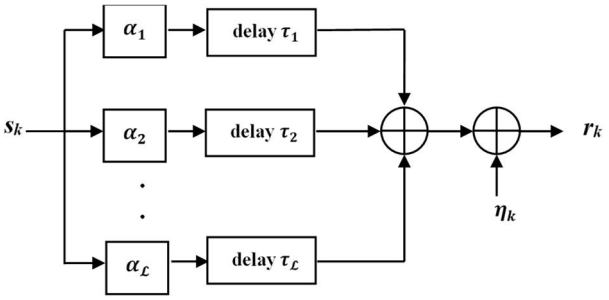

FIGURE 13. Multipath slow Raleigh fading channel model.

fading channels. In all derivations, the index j is omitted from the equations and a chip duration $T_c = 1$ is assumed for the sake of simplicity. The model channel with $\mathcal{L}$ independent paths is considered as illustrated in Fig. 13 with the l^{th} time delay τ_l, the l^{th} time complex channel coefficient α_l and the additive white Gaussian noise η_k, with an expectation value of zero and a variance of $N_0/2$. Assuming that the coefficients α_l are independent and identically distributed (i.i.d.), a slow Rayleigh fading channel and a maximum channel delay of $\tau_{max} \ll \beta$, the baseband received signal [27] channels is written as

$$r_k = \sum_{l=1}^{\mathcal{L}} \alpha_l s_{k-\tau_l} + \eta_k, \tag{19}$$

where $s_{k-\tau_l}$ is the channel delay version of the transmitted signal, s_k.

By substituting (3) and (19) in (9), the complex output correlation of the m^{th} transmitted bits in the n^{th} group at the receiver side can be expressed as (20), as shown at the top of the next page, where $x_{m,k-\tau_l}$, is the delay version of the m^{th} orthogonal chaotic vector, $\eta_{k+(m-1)\beta}$ and $\eta_{k+M\beta+(n-1)\beta}$ are the AWGN vectors added for each corresponding reference and information signal respectively and $(.)*$ is the conjugate function. Notice that the orthogonal chaotic signal $x_{m,k-\tau_l}$ is the same for each MN correlation.

Since the signals $x_{m,k-\tau_l}$ and $x_{u,k-\tau_l}$ are orthogonal, the following expression is used

$$\sum_{k=0}^{R-1} x_{m,k}x_{u,k} = 0, \quad m \neq u. \tag{21}$$

From (20) and (21), the m^{th} decision variable for the first group (n = 1) can be written as

$$\begin{aligned} D_m &= \Re e\left(Z\left(1,m\right)\right) \\ &= \Re e\left(\frac{1}{\sqrt{M}} d_m \sum_{k=0}^{\beta-1}\sum_{l=1}^{\mathcal{L}} |\alpha_l|^2 x_{m,k-\tau_l}^2 \right. \\ &\quad + \frac{1}{\sqrt{M}} \sum_{k=0}^{\beta-1}\sum_{u=1}^{M} d_u \sum_{l=1}^{\mathcal{L}} \alpha_l x_{u,k-\tau_l}\eta_{k+(m-1)\beta}^* \\ &\quad \left. + \sum_{k=0}^{\beta-1}\sum_{l=1}^{\mathcal{L}} \alpha_l^* x_{m,k-\tau_l}\eta_{k+M\beta} + \sum_{k=0}^{\beta-1} \eta_{k+(m-1)\beta}^*\eta_{k+M\beta}\right), \end{aligned} \tag{22}$$

$$Z(n,m)=\sum_{\mathrm{k}=0}^{\beta-1}\left(\begin{array}{c}\left(\sum_{\ell=1}^{\mathcal{L}}\alpha_\ell \mathrm{x}_{\mathrm{m,k}-\tau_\ell}+\eta_{\mathrm{k}+(\mathrm{m}-1)\beta}\right)^{*}\\ \times\left(\frac{1}{\sqrt{\mathrm{M}}}\sum_{\mathrm{u}=1}^{\mathrm{M}}\mathrm{d}_{\mathrm{u}+(\mathrm{n}-1)\mathrm{M}}\sum_{\mathrm{l}=1}^{\mathcal{L}}\alpha_\ell \mathrm{x}_{\mathrm{u,k}-\tau_\ell}+\eta_{\mathrm{k}+\mathrm{M}\beta+(\mathrm{n}-1)\beta}\right)\end{array}\right),\quad m=1,\ldots,M,\ n=1,\ldots,N, \tag{20}$$

where $\mathcal{R}e(.)$ is the real component of the complex sequence and $\eta^{*}_{\mathrm{k}+(\mathrm{m}-1)\beta}$ is the conjugate of $\eta_{\mathrm{k}+(\mathrm{m}-1)\beta}$. The first term in (22) represents the m^{th} desired data d_m, while all the remaining terms represent the noise and interference signals. Since the decision variables in all the m^{th} bits are identical, a Gaussian approximation (GA) method is applied to the first bit ($m = 1$) only. The BER of OFDM-OCVSK is expressed in terms of the complementary error function (*erfc*) as

$$\mathrm{BER}=\frac{1}{2}\mathrm{erfc}\left(\left[\frac{2\mathrm{V}(\mathrm{D}_1)}{\mathrm{E}(\mathrm{D}_1)^2}\right]^{-\frac{1}{2}}\right), \tag{23}$$

where $erfc(\lambda)=\frac{2}{\sqrt{\pi}}\int_{\lambda}^{\infty}e^{-t^2}dt$, V(.) the variance and E(.) the expectation function. The average value of the decision variable D_1 is the average of the first term in (22) for $m = 1$, since all the remaining terms are AWGNs with zero mean. With $d_m = +1$, therefore, $\mathrm{E}(\mathrm{D}_1)$ can be written as

$$E(D_1)=\frac{1}{\sqrt{M}}\sum\nolimits_{k=0}^{\beta-1}x_{1,k}^2. \tag{24}$$

For long spreading factors β, the bit energy E_b is virtually unchanged for all frames [33]. The term $\sum_{k=0}^{\beta-1}x_{1,k}^2$ can then be rewritten in terms of E_b to $\sum_{k=0}^{\beta-1}x_{1,k}^2=\mathrm{NME_b}/(\mathrm{N}+\mathrm{M})$ and then substituted in (24) to become

$$E(D_1)=\frac{\sqrt{M}N}{N+M}E_b\sum\nolimits_{l=1}^{\mathcal{L}}|\alpha_l|^2. \tag{25}$$

Assuming all terms in (25) are independent random variables and all mean square values of the u^{th} orthogonal chaotic vectors $E(x_{u,k}^2)$ are equal ($E(x_{1,k}^2)\approx E(x_{2,k}^2)\approx\ldots\approx E(x_{M,k}^2)$), the variance of the decision variable D_1 is given by

$$V(D_1)=\beta\frac{N_0}{2}\sum_{l=1}^{\mathcal{L}}|\alpha_l|^2E\left(x_{1,k}^2\right)+\beta\frac{N_0}{2}\sum\nolimits_{l=1}^{\mathcal{L}}|\alpha_l|^2E\left(x_{1,k}^2\right)+\beta\frac{N_0^2}{4} \tag{26}$$

With $E\left(x_{1,k}^2\right)=\frac{NE_b}{(N+M)\beta}$, (26) can be rearranged in terms of E_b to

$$V(D_1)=N_0\sum\nolimits_{l=1}^{\mathcal{L}}|\alpha_l|^2\frac{NME_b}{(N+M)}+\beta\frac{N_0^2}{4}. \tag{27}$$

Substituting (25) and (27) in (23), the BER of the OFDM-OCVSK system under multipath slow Rayleigh fading channel is given by

$$\mathrm{BER_{OFDM-OCVSK}}=\frac{1}{2}\mathrm{erfc}\left(\left[\frac{2(\mathrm{N}+\mathrm{M})}{\mathrm{N}\Omega_\mathrm{b}}+\frac{\beta(\mathrm{N}+\mathrm{M})^2}{2\mathrm{MN}^2\Omega_b^2}\right]^{-\frac{1}{2}}\right), \tag{28}$$

where $\Omega_\mathrm{b}=\sum_{l=1}^{\mathcal{L}}\alpha_\ell^2E_b/N_0$. The average BER over the probability distribution function (PDF) of Ω_b can then be written as

$$\overline{BER}=\frac{1}{2}\int_0^{\infty}\mathrm{erfc}\left(\left[\frac{2\,(\mathrm{N}+\mathrm{M})}{\mathrm{N}\Omega_\mathrm{b}}+\frac{\beta\,(\mathrm{N}+\mathrm{M})^2}{2\mathrm{MN}^2\Omega_\mathrm{b}^2}\right]^{-\frac{1}{2}}\right)\times\mathrm{f}(\Omega_\mathrm{b})\,\mathrm{d}\Omega_\mathrm{b}, \tag{29}$$

with $f(\Omega_b)$ being the PDF of the instantaneous Ω_b that is given by [25]:

$$f(\Omega_b)=\sum\nolimits_{l}^{\mathcal{L}}\frac{1}{\bar{\Omega}_\ell}\left(\prod\nolimits_{j=1,j\neq\ell}^{l}\frac{\bar{\Omega}_\ell}{\bar{\Omega}_l-\bar{\Omega}_j}\right)e^{-\frac{\Omega_b}{\bar{\Omega}_l}}. \tag{30}$$

Here, $\bar{\Omega}_\ell$ is the average value of $\Omega_l=|\Omega_l|^2E_b/\mathrm{N}_0$, which is the l^{th} instantaneous SNR.

Moreover, the BER of the OFDM-OCVSK system under AWGN only is derived from (28) by setting $\sum_{l=1}^{\mathcal{L}}|\alpha_l|^2=1$ as

$$\mathrm{BER_{AWGN}}=\frac{1}{2}\mathrm{erfc}\left(\left[\frac{2(\mathrm{N}+\mathrm{M})}{\mathrm{N}}\frac{\mathrm{N}_0}{\mathrm{E_b}}+\frac{\beta(\mathrm{N}+\mathrm{M})^2}{2\mathrm{MN}^2}\frac{\mathrm{N}_0^2}{\mathrm{E_b^2}}\right]^{-\frac{1}{2}}\right). \tag{31}$$

V. SIMULATION RESULTS AND DISCUSSION

This section presents the simulation results of OFDM-OCVSK system under AWGN and multipath Rayleigh fading channels and compares them with BER theory in (22) and (24) respectively. The simulation parameters used are M = (2, 4, 8, 16 and 32), N_{FFT} = (32, 64, 128, 256), $N=N_{FFT}-M$ and the guard interval $N_{guard}=0.25N_{FFT}$ = (8, 16, 32, 64).

A. AWGN CHANNEL

Fig. 14 shows the BER performance of an OFDM-OCVSK system under an AWGN channel with $N_{FFT}=128$, $\beta=50$ and M = 2, 4, 8 and 16. For constant subcarrier numbers N_{FFT}, the values of N are 126, 124, 120 and 112 for $M = 2, 4, 8, 16$, respectively. The results are also compared

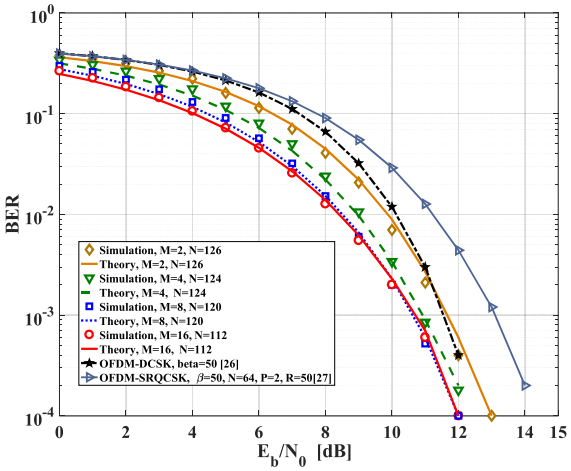

FIGURE 14. BER performance of OFDM-OCVSK systems with $N_{FFT} = 128$, $\beta = 50$ and $M = 2, 4, 8, 16$ under an AWGN channel. The results are also compared with OFDM-DCSK and OFDM-SRQCSK.

with OFDM-DCSK [32] ($N_{FFT} = N = 128$ and $\beta = 50$) and OFDM_SRQCSK [33] ($N_{FFT} = 128$, $\beta = 50$, P = 2, R = 50 and N = 64).

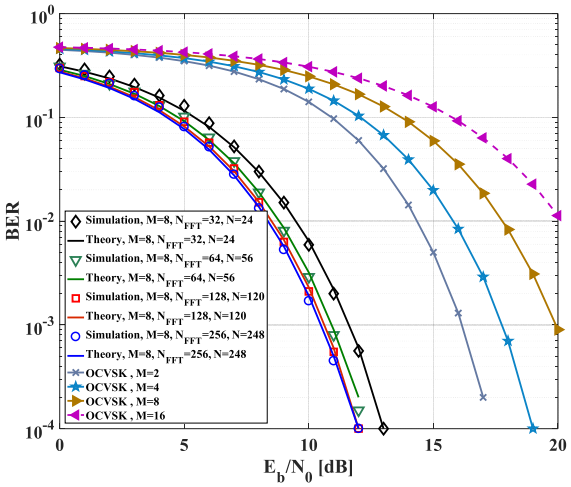

FIGURE 15. BER performance of OFDM-OCVSK systems with $M = 8$, $\beta = 50$ and $N_{FFT} = 32, 64, 128$ and 256 under AWGN channel. The results are also compared with OCVSK with $M = 2, 4, 8$ and 16.

In Fig. 15, the BER performance of OFDM-OCVSK with different subcarrier numbers is tested and compared with OCVSK for $M = 2, 4, 8, 16$, for $\beta = 50$ and for different spreading factors β (100, 150, 200, 250, 300).

In all figures, the simulation results are compared with the analytic expression in (21). Notice that increasing M values will enhance the BER performance up to a certain limit, as is shown in Fig. 16. Upward of this limit, the BER performance will decrease again. The optimum value for M depends on β, N_{FFT} and SNR. For certain values of M, any increase in N_{FFT} will improve the BER performance, with this improvement factor decreasing for large values of N_{FFT}. For example, with $\beta = 50$, M = 8 and BER = 10^{-3}, the resulting SNR values are 11.61, 11.00, 10.62 and 10.48 dB for $N_{FFT} = 32$, 64, 128 and 256 respectively. Therefore, increasing the subcarrier

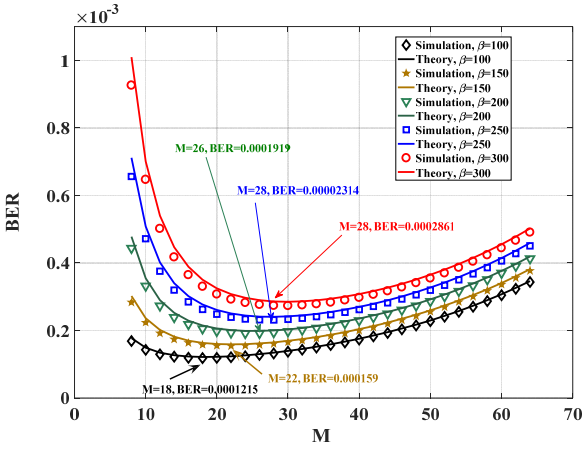

FIGURE 16. BER performance of OFDM-OCVSK systems with different M values under AWGN channel. Further parameters are: $N_{FFT} = 256$, SNR = 12 dB and $\beta = 100$, 150, 200, 250 and 300. The selection arrows refer to those values of M with minimum BER for a given β.

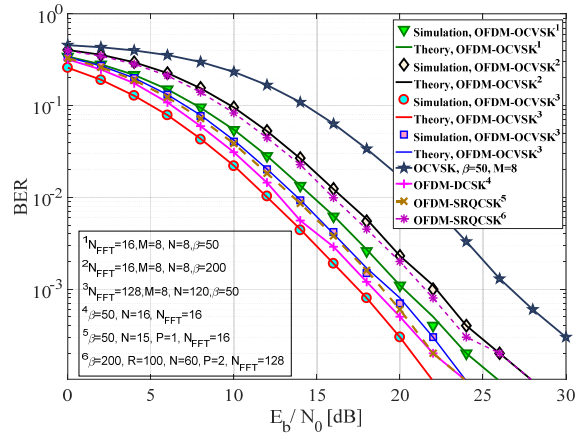

FIGURE 17. BER performance of OFDM-OCVSK under multipath fading channel for $N_{FFT} = 16$ and 128 and $\beta = 50$ and 100. The results are compared with OCVSK, OFDM-SRQCSK and OFDM-DCSK systems.

number from 128 to 256 will only enhance the SNR gain by about 0.14 dB. The results also clearly show that OFDM-OCVSK will enhance the BER performance in comparison with OFDM-DCSK [32] and OFDM-SRQCSK [33] for the same number of subcarriers and β values. For M = 8, for example, there is an SNR gain of about 1 dB and 2 dB when compared with OFDM-DCSK and OFDM-SPQCSK. The BER gain of combined OFDM with OCVSK systems as compared to pure OCVSK systems is also shown in Fig. 15. For example, setting M = 8 and $\beta = 50$ results in a gain of about 8 dB at $N_{FFT} = 32$. Furthermore, the figure shows that the BER simulation and the theory results compare well to each other.

B. MULTIPATH RAYLEIGH FADING CHANNEL

In this simulation, the results for a two-path Rayleigh fading channel are presented using average power levels of $E(\alpha_1^2) = 2/3$ and $E(\alpha_2^2) = 1/3$ and delay values of $\tau_1 = 0$ and

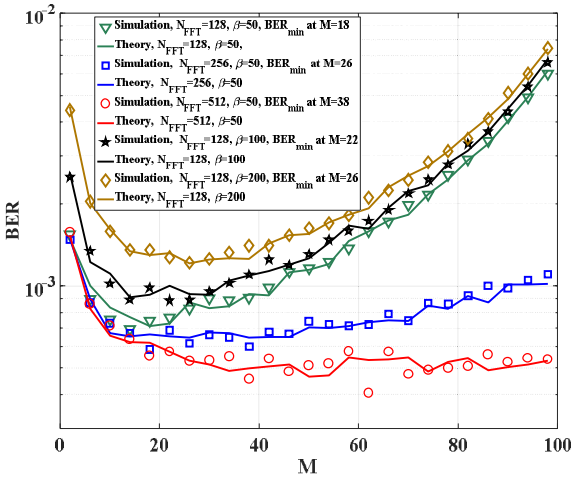

FIGURE 18. BER performance of OFDM-OCVSK versus M values under multipath fading channel for NFFT = 128, 256 and 512 and $\beta = 50$, 100 and 200.

$\tau_2 = 2\ T_c$ for each path respectively. Fig. 17 shows the BER performance of the OFDM-OCVSK under a multipath fading channel with M = 8, N_{FFT} = 32 and 128, and $\beta = 50$ and 200. The results are compared with OCVSK, OFDM-DCSK and OFDM-SRQCSK systems. Also, the simulation and analytic BER values of OFDM-OCVSK systems are compared. From this figure it can be seen that increasing N_{FFT} by increasing N and fixed M = 8 will enhance the performance of BER. For example, an increase of N_{FFT} from 16 to 128 will enhance the SNR gain by about 2 dB when M = 8, and β = 50 and 200 at BER = 10^{-3} is chosen. Similarly, decreasing the spread factor β from 200 to 50 will enhance the SNR gain by about 2 dB at a BER = 10^{-3}. OFDM-OCVSK in general results in better BER performance than OCVSK systems. The performance of an OFDM-OCVSK system with $N_{FFT} = 16$, $\beta = 200$ and M = 8 shows approximately the same behavior as that of an OFDM-SRQVSK with N_{FFT} = 128, P = 2, R = 100 and β = 200. While for the same environment β = 50, $N_{FFT} = 16$, the performance of OFDM-DCSK is better than OFDM-OCVSK (M = 8, N = 8) and OFDM-SRQCSK (P = 1, N = 15) by an SNR gain of about 2 and 1dB respectively. In general, the BER performance of OFDM-OCVSK systems for large N is better than both OFDM-DCK and OFDM-SRQCSK systems. Fig. 18 shows simulation and analytic BER comparisons of OFDM-OCVSK systems versus M for different N_{FFT} (228, 256 and 512) and β (50, 100 and 200) values. The increase of M enhances the BER performance up to a certain level after which the minimum BER degrades again. The level of M that gives minimum BER and hence optimal results depends on N_{FFT}, SNR and β values. For example, with N_{FFT} = 128 and β = 50 the minimum BER value occurred at M = 18. Changing β to a value of 100 leads to a minimum BER at M = 22. Of course increasing β will enhance the orthogonality of chaotic signals and carry more bits on the same time slot but on the other hand will need more SNR to get the same BER performance. Increasing N_{FFT} will enhance the BER performance at a falling rate as N_{FFT} is increased more and more.

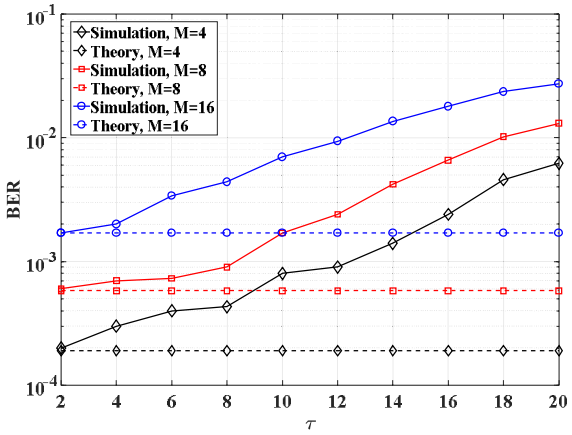

FIGURE 19. BER performance of the OFDM-OCVSK system versus τ under multipath fading channel with $\beta = 50$, M = 4, 8, 16 and $E_b/N_0 = 20$ dB.

Fig. 19 shows the effect of the multipath time delay τ on the BER performance of OFDM-OCVSK for two path Rayleigh fading channels with $\beta = 50$, $M = 4, 8, 16$, $NFFT = 128$, $N = 128 - M$ and $E_b/N_0 = 20\ dB$. An increase of τ will increase the intersymbol interference (ISI) and degrade the BER performance. The analytic expression does not fully match the simulation results because of assumed $\tau \ll \beta$ and thus neglect ion of ISI and independency of τ.

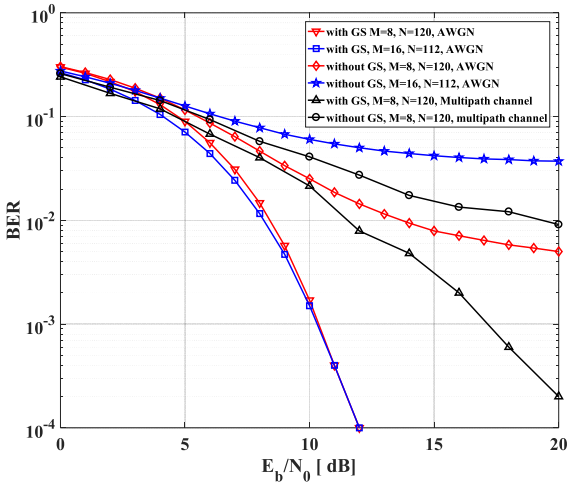

FIGURE 20. BER performance of OFDM-OCVSK with 128 subcarriers and $M = 8$ or 16 chaotic generators, each of length $\beta = 50$, with and without additional Gram-Schmidt processing.

The BER performance of OFDM-OCVSK for orthogonal chaotic sequences generated by the GS algorithm as compared to the non-orthogonal sequences generated by different initial conditions under AWGN and multipath fading channels is shown in Fig. 20. The results clearly show that the BER performance of the system is enhanced with the Gram-Schmidt algorithm under both channel models, AWGN and multipath Rayleigh fading channel.

VI. CONCLUSION

The proposed system combines OFDM and OCVSK in a manner that substantially improves the spectral efficiency, the bit energy and the BER performance of OCVSK systems. The derivation of the information rate, the energy-saving enhancements and the DBR factors compared with OCVSK systems was presented. The results show that, for large values of N, the IRE and ESE factors approach $M \times 100\%$ and $M/(M+1) \times 100\%$ respectively. The system also approaches the DBR factors of OFDM-SRQCSK systems when large enough values of N are selected. The complexity of the proposed system on the transmitter side was compared with OFDM-DCSK. For the same number of transmitted bits, the results show a significant reduction in the number of complex multiplications required for the OFDM-OCVSK compared with the OFDM-DCSK system. The simulation and analytic BER performance of the OFDM-OCVSK systems proposed under an AWGN and multipath Rayleigh fading channels were presented. The results show a good level of overlap between theory and the results of the simulation. The comparison with OFDM-DCSK and OFDM-SRQCSK shows that the proposed system could be a promising candidate for non-coherent multicarrier spread spectrum systems in future wireless communication systems.

REFERENCES

[1] G. Kaddoum, "Wireless chaos-based communication systems: A comprehensive survey," *IEEE Access*, vol. 4, pp. 2621–2648, May 2016.

[2] Y. Xia, C. K. Tse, and F. C. M. Lau, "Performance of differential chaos-shift-keying digital communication systems over a multipath fading channel with delay spread," *IEEE Trans. Circuits Syst., II, Exp. Briefs*, vol. 51, no. 12, pp. 680–684, Dec. 2004.

[3] J. Yu and Y.-D. Yao, "Detection performance of chaotic spreading LPI waveforms," *IEEE Trans. Wireless Commun.*, vol. 4, no. 2, pp. 390–396, Mar. 2005.

[4] M. Z. Hasan, I. Idris, A. F. M. N. Uddin, and M. Shahjahan, "Performance analysis of a coherent chaos-shift keying technique," in *Proc. 15th Int. Conf. Comput. Inf. Technol. (ICCIT)*, 2012, pp. 249–254.

[5] G. Kolumban, B. Vizvári, W. Schwarz, and A. Abel, "Differential chaos shift keying: A robust coding for chaos communication," in *Proc. NDE*, vol. 96, 1996, pp. 87–92.

[6] Z. Zhou, T. Zhou, and J. Wang, "Exact BER analysis of differential chaos shift keying communication system in fading channels," in *Proc. 4th Int. Conf. Wireless Commun., Netw. Mobile Comput.*, 2008, pp. 1–4.

[7] T. J. Wren and T. C. Yang, "Orthogonal chaotic vector shift keying in digital communications," *IET Commun.*, vol. 4, no. 6, pp. 739–753, Apr. 2010.

[8] G. Kolumban, M. P. Kennedy, G. Kis, and Z. Jako, "FM-DCSK: A novel method for chaotic communications," in *Proc. IEEE Int. Symp. Circuits Syst. (ISCAS)*, vol. 4, May 1998, pp. 477–480.

[9] M. P. Kennedy and G. Kolumbán, G. Kis, and Z. Jákó, "Performance evaluation of FM-DCSK modulation in multipath environments," *IEEE Trans. Circuits Syst. I, Fundam. Theory Appl.*, vol. 47, no. 12, pp. 1702–1711, Dec. 2000.

[10] Z. Galias and G. M. Maggio, "Quadrature chaos-shift keying: Theory and performance analysis," *IEEE Trans. Circuits Syst. I, Fundam. Theory Appl.*, vol. 48, no. 12, pp. 1510–1519, Dec. 2001.

[11] H. Yang, W. K. S. Tang, and G. Chen, "System design and performance analysis of orthogonal multi-level differential chaos shift keying modulation scheme," *IEEE Trans. Circuits Syst. I, Reg. Papers*, vol. 63, no. 1, pp. 146–156, Jan. 2016.

[12] H. Yang and G.-P. Jiang, "High-efficiency differential-chaos-shift-keying scheme for chaos-based noncoherent communication," *IEEE Trans. Circuits Syst. II, Exp. Briefs*, vol. 59, no. 5, pp. 312–316, May 2012.

[13] H. Yang and G.-P. Jiang, "Reference-modulated DCSK: A novel chaotic communication scheme," *IEEE Trans. Circuits Syst., II, Exp. Briefs*, vol. 60, no. 4, pp. 232–236, Apr. 2013.

[14] G. Zhang, Y. Wang, and T.-Q. Zhang, "A novel QAM-DCSK secure communication system," in *Proc. Int. Congr. Image Signal Process. (CISP)*, Dalian, China, 2014, pp. 994–999.

[15] L. Wang, G. Cai, and G. R. Chen, "Design and performance analysis of a new multiresolution M-ary differential chaos shift keying communication system," *IEEE Trans. Wireless Commun.*, vol. 14, no. 9, pp. 5197–5208, May 2015.

[16] G. Kaddoum and F. Gagnon, "Design of a high-data-rate differential chaos-shift keying system," *IEEE Trans. Circuits Syst., II, Exp. Briefs*, vol. 59, no. 7, pp. 448–452, Jul. 2012.

[17] W. K. Xu, L. Wang, and G. Kolumbán, "A novel differential chaos shift keying modulation scheme," *Int. J. Bifurcation Chaos*, vol. 21, pp. 799–814, Mar. 2011.

[18] K. Thilagam and K. Jayanthi, "A novel chaos based modulation scheme (CS-QCSK) with improved BER performance," in *Proc. Conf CSIT-Comput. Sci. (CONECO)*, 2012, pp. 45–59.

[19] H. Yang, G.-P. Jiang, and J. Duan, "Phase-separated DCSK: A simple delay-component-free solution for chaotic communications," *IEEE Trans. Circuits Syst., II, Exp. Briefs*, vol. 61, no. 12, pp. 967–971, Sep. 2014.

[20] G. Kaddoum, E. Soujeri, C. Arcila, and K. Eshteiwi, "I-DCSK: An improved noncoherent communication system architecture," *IEEE Trans. Circuits Syst., II, Exp. Briefs*, vol. 62, no. 9, pp. 901–905, May 2015.

[21] G. Kaddoum, E. Soujeri, and Y. Nijsure, "Design of a short reference non-Coherent chaos-based communication systems," *IEEE. Trans. Commun.*, vol. 64, no. 2, pp. 680–689, Jan. 2016.

[22] T. Huang, L. Wang, and W. Xu, "Multilevel code-shifted differential-chaos-shift-keying system," *IET Commun.*, vol. 10, no. 10, pp. 1189–1195, 2016.

[23] M. Herceg, D. Vranjes, G. Kaddoum, and E. Soujeri, "Commutation code index DCSK modulation technique for high-data-rate communication systems," *IEEE Trans. Circuits Syst., II, Exp. Briefs*, to be published.

[24] E. Soujeri, G. Kaddoum, and M. Herceg, "Design of an initial condition-index chaos shift keying modulation," *Electron. Lett.*, vol. 54, no. 7, pp. 447–449, Apr. 2018.

[25] F. Lau, K. Cheong, and C. Tse, "Permutation-based DCSK and multiple-access DCSK systems," *IEEE Trans. Circuits Syst., II, Exp. Briefs*, vol. 50, no. 6, pp. 733–742, Jun. 2003.

[26] M. Herceg, G. Kaddoum, and D. Vranjes, "Permutation index DCSK modulation technique for secure multiuser high-data-rate communication systems," *IEEE Trans. Veh. Technol.*, vol. 67, no. 4, pp. 2997–3011, Apr. 2017.

[27] F. J. Escribano, G. Kaddoum, A. Wagemakers, and P. Giard, "Design of a new differential chaos-shift-keying system for continuous mobility," *IEEE Trans. Commun.*, vol. 64, no. 5, pp. 2066–2078, May 2016.

[28] M. Dawa, G. Kaddoum, and Z. Sattar, "A generalized lower bound on the bit error rate of DCSK systems over multi-path Rayleigh fading channels," *IEEE Trans. Circuits Syst.*, vol. 65, no. 3, pp. 321–325, Mar. 2018.

[29] W. Rao, L. Zhang, Z. Liu, and Z. Wu, "Efficient amplitude shift keying-aided orthogonal chaotic vector position shift keying scheme with QoS considerations," *IEEE Access*, vol. 5, pp. 14706–14715, 2017.

[30] G. Kaddoum, F. Gagnon, and F.-D. Richardson, "Design of a secure multi-carrier DCSK system," in *Proc. Int. Symp. Wireless Commun. Syst. (ISWCS)*, 2012, pp. 964–968.

[31] G. Kaddoum, F. Richardson, and F. Gagnon, "Design and analysis of a multi-carrier differential chaos shift keying communication system," *IEEE Trans. Commun.*, vol. 61, no. 8, pp. 3281–3291, Aug. 2013.

[32] S. Li, Y. Zhao, and Z. Wu, "Design and analysis of an OFDM-based differential chaos shift keying communication system," *J. Commun.*, vol. 10, no. 3, pp. 199–205, 2015.

[33] S. Fadhil Hasan, "Design and analysis of an OFDM-based short reference quadrature chaos shift keying communication system," *Wireless Pers. Commun.*, vol. 96, no. 2, pp. 2205–2222, 2017.

[34] G. Kaddoum, F.-D. Richardson, S. Adouni, F. Gagnon, and C. Thibeault, "Multi-user multi-carrier differential chaos shift keying communication system," in *Proc. Int. Wireless Commun. Mobile Comput. Conf. (IWCMC)*, 2013, pp. 1798–1802.

[35] G. Kaddoum and F. Shokraneh, "Analog network coding for multi-user multi-carrier differential chaos shift keying communication system," *IEEE Trans. Wireless Commun.*, vol. 14, no. 3, pp. 1492–1505, Mar. 2015.

[36] G. Kaddoum, "Design and performance analysis of a multiuser OFDM based differential chaos shift keying communication system," *IEEE Trans. Commun.*, vol. 64, no. 1, pp. 249–260, Jan. 2016.
[37] H. Yang, W. K. S. Tang, G. Chen, and G.-P. Jiang, "Multi-carrier chaos shift keying: System design and performance analysis," *IEEE Trans. Circuits Syst. I, Reg. Papers*, vol. 64, no. 8, pp. 2182–2194, Aug. 2017.
[38] S. Venkatesh and P. Singh, "Performance analysis of OCV based non coherent MA chaotic communication system with adaptive multi user receivers," in *Proc. Int. Conf. Devices Commun. (ICDeCom)*, 2011, pp. 1–5.
[39] G. Kaddoum, F. Gagnon, P. Chargé, and D. Roviras, "A generalized BER prediction method for differential chaos shift keying system through different communication channels," *Wireless Pers. Commun.*, vol. 64, no. 2, pp. 425–437, 2012.

FADHIL S. HASAN was born in Baghdad, Iraq, in 1978. He received the B.Sc. degree in electrical engineering and the M.Sc. degree in electronics and communication engineering from Mustansiriyah University, Iraq, in 2000 and 2003, respectively, and the Ph.D. degree in electronics and communication engineering from Basrah University, Iraq, in 2013.

In 2005, he joined the Faculty of Engineering, Al-Mustansiryah University, Baghdad, where he is currently an Assistant Professor. His recent research activities cover wireless communication systems, multicarrier systems, wavelet-based OFDM, MIMO systems, speech signal processing, chaotic modulation, FPGA, and xilinx system generator-based communication systems.

ALEJANDRO A. VALENZUELA was born in San Carlos de Bariloche, Argentina, in 1963. He received the Dipl.Ing. and Dr.Ing. degrees in electrical engineering from the Technische Universität München, Germany, in 1987 and 1992, respectively.

In 1988, he joined the Research Institute of Siemens AG, Munich, where he was involved in circuit measurements and diagnostics, the development of contactless measurement methods, and the application of high-temperature superconducting thin films. From 1992 to 1993, he was involved in the development of broadband switching systems and from 1994 to 2001, as the Head of the development services broadband peripheral subsystems and line interface circuits hardware in the organizations Information and Communication Networks and Information and Communication Mobile at Siemens AG, Munich. Since 2001, he has been a Full Professor and the Head of the Communications Laboratory, Hochschule Bonn-Rhein-Sieg University of Applied Sciences, Germany.